Available online at www.sciencedirect.com
ScienceDirect
Nuclear Instruments and Methods in Physics Research B 255 (2007) 259–264
NIM B
Beam Interactions with Materials & Atoms
www.elsevier.com/locate/nimb

Crater annihilation on silver by cluster ion impacts

K.O.E. Henriksson [a,b,*], K. Nordlund [b], J. Keinonen [b]

[a] Department of Reactor Physics, Royal Institute of Technology, SE-10691 Stockholm, Sweden
[b] Accelerator laboratory, University of Helsinki, P.O.Box 43, FI-00014 University of Helsinki, Finland

Available online 14 December 2006

Abstract

Using the MD/MC-CEM potential we have investigated the impacts of 20 keV Ag_{13} cluster ions on (0 0 1) silver surfaces having one initial crater. This one was made in the zeroth ion impact. The degree of annihilation of the initial crater was investigated as a function of the lateral distance r_i between the crater and the ion. The impact points were selected randomly inside a circular area with a radius of 75 Å centered on the crater. To reduce the total number of simulations, the circular area was divided into annuli. The initial and final atomic positions in the impact simulations were analyzed and the degree of annihilation of the initial crater was determined. The results indicate that for $r \lesssim 60$ Å there is a net growth of the initial crater, and for distances $r \in (60, 80)$ Å there is a small net filling of the crater.

PACS: 36.40.−c; 61.80.Lj; 83.10.Mj

Keywords: Cluster ion; Heavy ion; Irradiation; Crater formation; Silver; Molecular dynamics simulations

1. Introduction

For anyone equipped with a good pair of binoculars and an intuitive understanding of collision physics, it is not difficult to believe that some incomplete circular structures embedded into the surface of the Moon constitute the remains of craters partly destroyed by later meteorite impacts. Although ion-induced nanoscopic craters on solids are many magnitudes smaller in size, the essential features – such as size and shape – obey similar laws as for the macroscopic craters (see [1] for references). Therefore it is not surprising that also nanoscopic craters can be partly or fully destroyed by later projectile impacts.

Irradiation experiments on dense metals show that xenon ions with energies between 50 and 400 keV incident on gold give rise to craters as well as destroy earlier ones – either completely or partly – in a single step [2,3]. The probability that a single ion was able to cause the formation of a crater was found to be 2–5%, leading to the conclusion that most ions annihilate craters instead of creating new ones. With the assumption that all ions are capable of annihilating craters, Donnelly and Birtcher [3] conclude from an analysis of transmission electron microscopy (TEM) images that a single xenon had an annihilation cross-section of $\sigma_a = 1/(f\tau) \approx 85\ \mathrm{nm}^2$ for small craters with a radius of $R'_s \approx 22$ Å. Here $f = 2.4 \times 10^{15}\ \mathrm{m}^{-2}\,\mathrm{s}^{-1}$ is the ion flux and $\tau = 4.9$ s is the lifetime of the craters present on the area under investigation. The interpretation of this is, according to the authors, that an ion impacting within a distance of about 50 Å of a small crater, will annihilate this crater. This distance corresponds to $2.3R'_s$.

In this study we have investigated the crater annihilation efficiency of 20 keV Ag_{13} cluster ions incident on (0 0 1) Ag surfaces displaying one initial (initial) crater with the radius $R_s \approx 28$ Å. The present results indicate that for a lateral crater–ion distance of $r \lesssim 60\ \text{Å} \approx 2.1R_s$ there is actually a net growth of the initial crater, and for distances $r \in (60, 80)\ \text{Å} \approx (2.1R_s, 2.9R_s)$ there is a small net filling of the crater.

* Corresponding author. Tel.: +46 8 5537 8197; fax: +46 8 5537 8465.
E-mail address: krihen@kth.se (K.O.E. Henriksson).

0168-583X/$ - see front matter
doi:10.1016/j.nimb.2006.11.037

2. Computational methods

2.1. Simulation for the development of the initial crater

For the simulation of the development of the initial crater, a face-centered cubic (FCC) silver target with 72 conventional unit cells in the x and y directions, and 36 cells in the z direction, was created. This gave a total of 746,496 atoms. The lattice parameter a at 300 K and zero pressure was used, giving the substrate dimensions $L_x = L_y \approx 297$ Å and $L_z = 148$ Å. The same a was used to create the impinging icosahedral cluster, which was randomly rotated and placed at about 25 Å above the surface. Periodic boundary conditions were used in the x and y directions. This left two open surfaces in the z direction. To remove one of these, the atoms in a 5 Å thick region at the lower z boundary were kept fixed at all times. In this way the lower surface of the target was removed, leaving only one true surface.

At the start of the simulation, a total energy of 20 keV (1.5 keV/atom) was given to the cluster. The momentum vector was antiparallel to the z axis. The target was constructed using the lattice parameter $a = 4.12$ Å corresponding to 300 K, but the simulation cell was not equilibrated at this temperature before the irradiation event. Therefore the cell had an initial temperature of 0 K. In order to model the dissipation of heat and pressure into the medium surrounding the cascade, the Berendsen temperature control method [4] was used: The atoms in a $2a$ thick region directly adjacent to the layer of fixed atoms at the bottom of the simulation cell – and the atoms at all the periodic boundaries – were subjected to velocity scaling. In this way the temperature in these regions tended to 300 K.

The Corrected Effective Medium potential tailored for molecular dynamics and Monte Carlo calculations – abbreviated MD/MC-CEM – was used for the calculations. See [5–9] for the complete decsription of the CEM and MD/MC-CEM potentials. The form used in the present calculations is based on the work by Kelchner et al. [10]. The MD/MC-CEM potential does not rely on empirical inputs to the same extent as the Embedded Atom Method potential [11–15], which also is an effective medium potential. The MD/MC-CEM potential is fitted to *ab initio* bulk and experimental dimer properties, and should therefore give a better description of *e.g.* surface phenomena than the EAM potential.

In the simulations, the loss of energy due to collisions with electrons was accounted for by using the electronic stopping function constructed by Ziegler, Biersack and Littmark [16]. The stopping was applied to all atoms with an energy of 5 eV or higher.

The energy deposited by the ion heated the target to an average temperature of 220 K after the first 10 ps. The simulation was ended at 50 ps, when the cascade had subsided. The system was then equilibrated to 300 K during an additional simulation time of 2 ps. After this, all sputtered atoms were removed.

2.2. Simulation of ion–crater interaction

For the simulations of cluster ions impacting on the initial crater, the same conditions for atom fixing and cluster position as above were used. However, the regions where the temperature was controlled was enlarged: the thickness of the region above the fixed layers was increased to $8a$, and the thickness of the regions at the side walls was increased to $4a$. This was done in order to ensure a very effective dampening of the pressure wave caused by the ion impact. In addition, the simulation time was extended to 80 ps to make sure that the system had time to be relaxed at 300 K for tens of picoseconds.

The impact points for the 13-atom randomly oriented silver clusters were selected inside a circular area with the radius 75 Å centered on the initial crater. To reduce the total number of simulations, the circular area was divided into annuli with thickness of $d = 5$ Å. The distance from the initial crater to any annulus – the "binned" lateral distance – was

$$r_i = \left(i + \frac{1}{2}\right) d, \tag{1}$$

with $i = 0, \ldots, 14$, resulting in $\min(r_i) = 0.5d = 2.5$ Å and $\max(r_i) = 14.5d = 72.5$ Å. In order to keep the number of simulations at a minimum, an impact probability of $p = N/A \times \pi d^2 = 0.49$ was selected. Since the area of each annulus was

$$A = \pi((i+1)^2 - i^2)d^2 = \pi(2i+1)d^2. \tag{2}$$

this resulted in

$$N = p(2i+1) \approx i \tag{3}$$

ions per annulus.

Before any simulation started the substrate was shifted in the x and y directions, such that the ion always impacted at $(x, y) = (0, 0)$, and the initial crater was located at $(r\cos\theta, r\sin\theta)$. The "direct" lateral distance $r \in [0, 75]$ Å and the angle $\theta \in [0, 2\pi)$ were chosen randomly.

2.3. Analysis of crater annihilation

The initial and final positions of the atoms were analyzed for vacancy clusters. The initial configuration always had one vacancy cluster, corresponding to the initial crater. The number of vacancies in this crater was denoted N_0. In the final configuration there were one or two craters. The one that intersected the initial crater was called "old". Any second crater was called "new". The number of vacancies in the old (new) crater was denoted M_1 (M_2).

The relative change in the size of the initial crater is defined as

$$f \equiv \frac{M_1 - N_0}{N_0}. \tag{4}$$

The relative change in total crater volume is

$$f_{\mathrm{V}} \equiv \frac{M_1 + M_2}{N_0}. \tag{5}$$

The removal fraction of the initial crater is equal to

$$f_{\mathrm{r}} \equiv \frac{N_{\mathrm{r}}}{N_0}, \tag{6}$$

where N_{r} is the number of vacancies that have been removed from the initial crater. This can be used as an intuitive measure of the filling-in of the initial crater, but it has to be kept in mind that any added – new – vacancies are not accounted for in this quantity.

The results from these calculations are obtained as a function of the binned and direct lateral distances r_{i} and r, respectively, between the cluster ion and the initial crater.

3. Results and discussion

3.1. The initial crater

Vacancy analysis of the initial crater showed that the topmost circular layer of the cluster contained 289 vacancies. Using a surface density of $\sigma = 2/a^2$, with $a = 4.12$ Å, the radius of the top layer becomes $R_{\mathrm{s}} = 27.9$ Å ≈ 28 Å. The depth of the crater is $h = 26.8$ Å. For a single linear-size measure of the crater the weighted average $(R_{\mathrm{s}} + 2h)/3 = 27.5$ Å ≈ 28 Å $\equiv R_{\mathrm{s}}$ may be used.

3.2. Change in the size of the initial crater

The final state of targets with a initial crater irradiated with a cluster ion is shown in Fig. 1, for several different crater–ion distances. The initial crater has not received

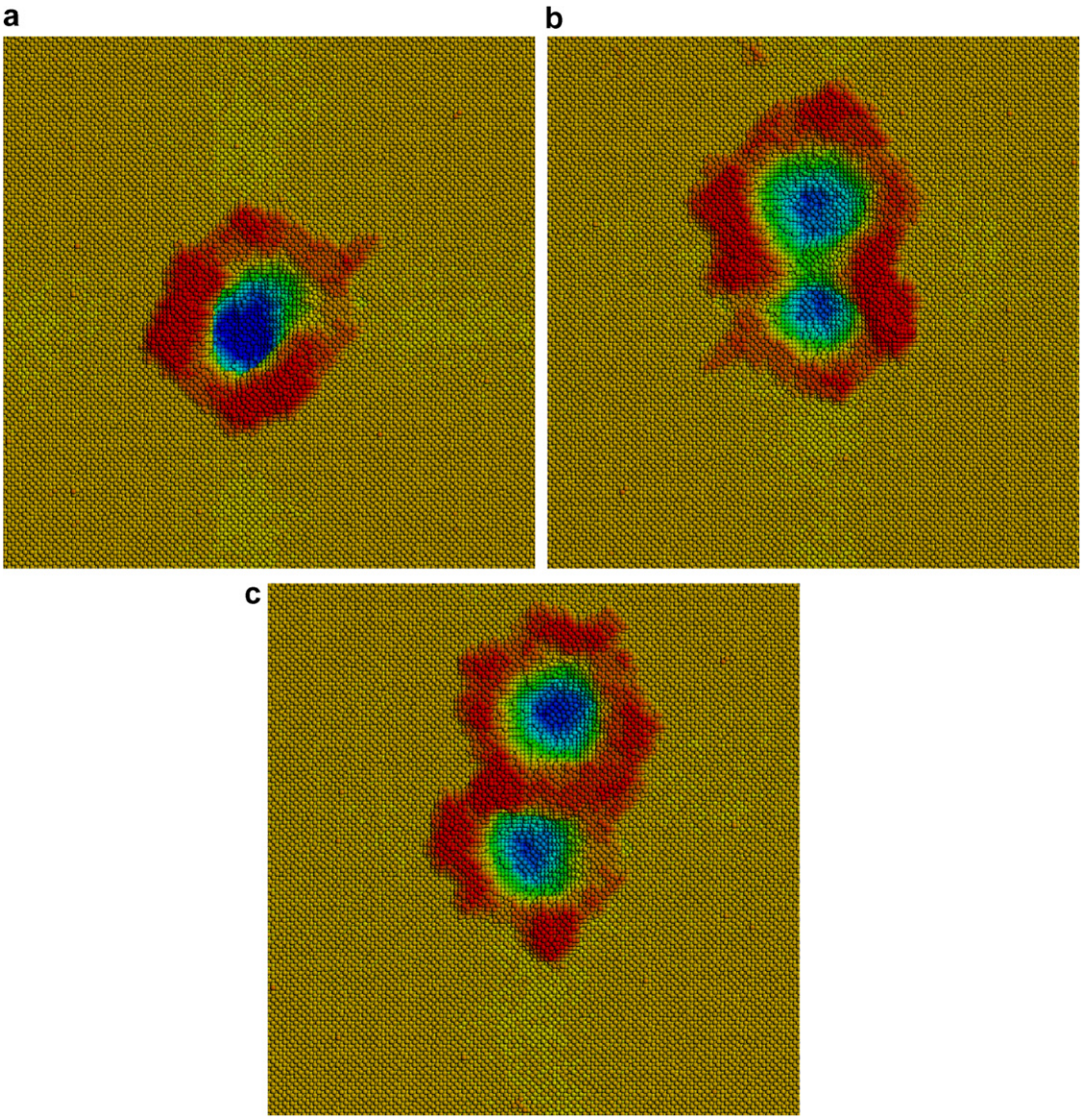

Fig. 1. Targets after a single-ion irradiation of the initial crater, for lateral crater–ion distances of (a) $r = 25$ Å, (b) $r = 50$ Å and (c) $r = 75$ Å.

much filling material. Instead a second crater intersecting the initial one is usually formed.

3.3. Relative change in the size of the initial crater, f

The relative change f in size of the initial crater is shown in Fig. 2 as a function of the binned and direct lateral distance between the crater and the incident ion. The incident ion will make the initial crater (i) smaller or (ii) larger, resulting in f taking both negative and positive values.

3.4. Relative change in total crater volume, f_V

The relative change f_V in the total crater volume is shown in Fig. 3. An ion incident on a point far from the initial crater will give rise to a similar crater as the initial one, resulting in f_V taking a maximum value close to 2.0.

3.5. Removal fraction of the initial crater, f_r

The removal fraction f_r of the initial crater is shown in Fig. 4. An ion incident on a point far from the initial crater will not be able to fill it substantially, resulting in f_r approaching 0.0. The estimate by Donnelly and Birtcher for 50–400 keV xenon ions incident on gold is also displayed. In this case the critical radius $2.3R'_s$ (mentioned in Section 1) for annihilation has first been converted to the dimensionless quantity 2.3 and then to the (dimensional) value $2.3R_s$. Please note the different crater radii R'_s and R_s.

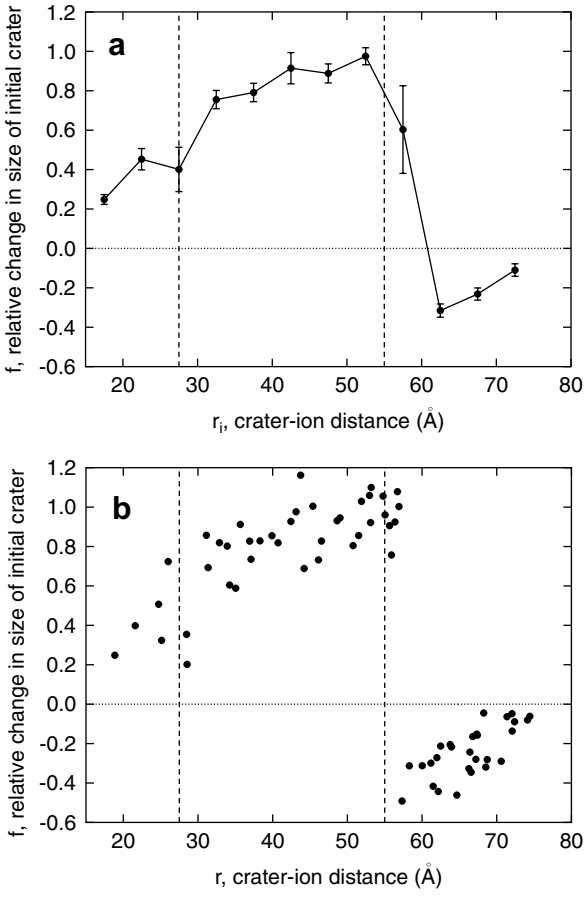

Fig. 2. Relative change in the size of the initial crater, as a function of the (a) binned and (b) direct lateral distance between the crater and the cluster ion. The broken line is a guide for the eye. The vertical lines mark integer multiples of the radius R_s of the initial crater. The data are from 68 simulations. Single data points have been given an uncertainty of 10%.

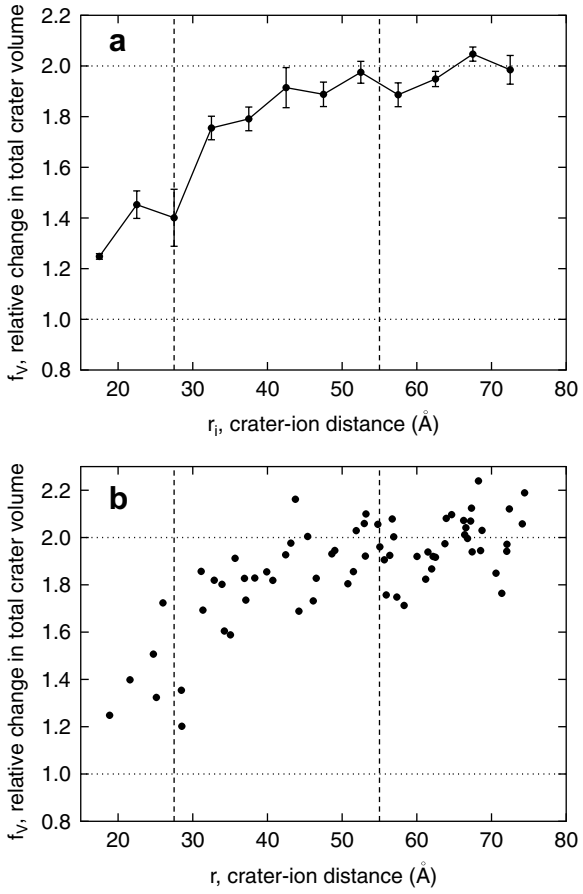

Fig. 3. Relative change in the total crater volume, as a function of the (a) binned and (b) direct lateral distance between the crater and the cluster ion. Other details are identical to those in Fig. 2.

3.6. Summary of findings

The results in Figs. 2 and 3 show that a cluster ion incident very close to the initial crater will not annihilate it, but instead make it somewhat larger. However, it should be kept in mind that "larger" does not necessarily mean a crater with larger radius or depth, but simply a crater (the initial one) with added vacancies at the bottom, on the sides, or in a surface cluster connected to it. The increase in volume of the initial crater is largest when the lateral distance between the cluster ion and the initial crater is about twice the radius of the latter one, *i.e.* for $r \approx 2R_s \approx 55$ Å.

When the distance is increased, the new crater becomes disconnected from the old one, which now receive filling material through the crater formation process initiated by the incident ion. As the distance is increased, the

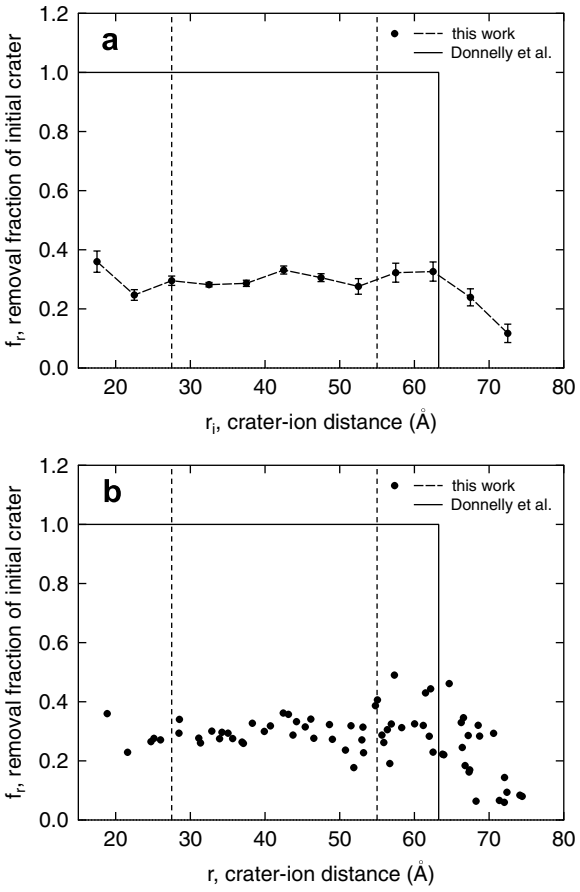

Fig. 4. Removal fraction of the initial crater, as a function of the (a) binned and (b) direct lateral distance between the crater and the cluster ion. The caption 'Donnelly et al.' refers to [3]. It should be noted that the scale of the y axis is different from those of the other figures. Other details are identical to those in Fig. 2.

interaction between the initial crater and the ion becomes weaker, resulting in decreased filling, and f approaching 0.0 for $r \approx 2.7R_s \approx 75$ Å. At the same time, the surface topography changes from two connected crater-like forms into two separate craters, which results in $f_V \approx 2.0$, see Fig. 3.

The intuitive measure for crater annihilation, f_r, plotted in Fig. 4, suggests that about 30% of the vacancies in the initial crater are destroyed when a cluster ion impacts at distances $r \in (0, 65)$ Å. The annihilation fraction then decreases to about 10% at a distance of about 75 Å. For larger distances, the value f_r must naturally approach 0.0. These results show some agreement with the estimate of Donnelly and Birtcher [3], who found that ions impacting at a lateral distance smaller than 2.3 times the crater radius would annihilate the initial crater, which had a radius of about $R'_s = 22$ Å. This converts to $f_r = 1$ for $r \in (0, 2.3R'_s)$ and $f_r = 0$ for $r > 2.3R'_s$, with unknown and possibly large uncertainties. The important quantity in the comparison is the critical distance r_c at which the annihilation ratio drops from nonzero to close to zero. The present results give $r_c \approx 70$ Å $\approx 2.5R_s$. Despite the differences in target materials and ion species and energies, the present results and that by Donnelly and Birtcher are in good agreement concerning r_c.

The main discrepancy between the present results and those of Donnelly and Birtcher [3] is the amount of filling or annihilation of the craters, despite the similar crater radii. The main reason for this is most likely the different ion types – atom *versus* cluster – and energies. The 20 keV Ag_{13} ions do not penetrate very deep into the Ag target. Instead they cause the excavation of a hemispherical region right at the surface. The displaced material is either ejected or deposited at the crater rim. In any case, there is not much molten material able to flow around and smooth out any neighboring crater. Similar effects occur when meteorites hit pre-existing craters on *e.g.* the Moon, since also in this case the "ion" (the meteorite) consists of many units common to both the projectile and the target. On the other hand, the 50–400 keV Xe ions have a range of 100–510 Å according to MDRANGE calculations [17], which is much larger than the radius $R'_s = 22$ Å of the corresponding (small) craters. The displaced hot target material below the surface has nowhere else to go but upwards to the surface. It is conceivable this material fills up the ion track and possibly spill up onto the surface. Seen from the initial direction of the ion the crater may seem partly or fully annihilated.

More results, with improved statistical significance and details of the annihilation and expansion of the initial crater will be published elsewhere.

4. Conclusions

Molecular dynamics simulations of Ag_{13} clusters incident on a Ag(0 0 1) surface at normal incidence show that initial craters (with a radius of about $R_s \approx 28$ Å) are made larger when the lateral distance r from the ion to the crater is $\approx 2R_s$ or smaller. For distances up to $\approx 2.7R_s$, the initial crater is partly annihilated, with the degree of annihilation decreasing in magnitude with increasing distance.

The molecular dynamics calculations presented in this article have been carried out in the CSC's computating environment. CSC is the Finnish IT center for science and is owned by the Ministry of Education.

References

[1] K. Nordlund, K.O.E. Henriksson, J. Keinonen, Appl. Phys. Lett. 79 (22) (2001) 3624.
[2] R.C. Birtcher, S.E. Donnelly, Phys. Rev. Lett. 77 (1996) 4374.
[3] S.E. Donnelly, R.C. Birtcher, Phys. Rev. B 56 (1997) 13599.
[4] H.J.C. Berendsen, J.P.M. Postma, W.F. van Gunsteren, A.D. Nola, J.R. Haak, J. Chem. Phys. 81 (1984) 3684.
[5] J.D. Kress, A.E. DePristo, J. Chem. Phys. 87 (1987) 4700.
[6] J.D. Kress, A.E. DePristo, J. Chem. Phys. 88 (1988) 2596.
[7] J.D. Kress, M.S. Stave, A.E. DePristo, J. Phys. Chem. 93 (1989) 1556.
[8] T.J. Raeker, A.E. DePristo, Phys. Rev. B 39 (1989) 9967.
[9] M.S. Stave, D.E. Sanders, T.J. Raeker, A.E. DePristo, J. Chem. Phys. 93 (1990) 4413.

[10] C. Kelchner, D. Halstead, L. Perkins, N. Wallace, A. DePristo, Surf. Sci. 310 (1994) 425, and references therein.
[11] M.S. Daw, M.I. Baskes, Phys. Rev. Lett. 50 (17) (1983) 1285.
[12] M.S. Daw, M.I. Baskes, Phys. Rev. B 29 (12) (1984) 6443.
[13] S.M. Foiles, M.I. Baskes, M.S. Daw, Phys. Rev. B 33 (12) (1986) 7983.
[14] M.S. Daw, Phys. Rev. B 39 (11) (1989) 7441.
[15] M.S. Daw, S.M. Foiles, M.I. Baskes, Mater. Sci. Rep. 9 (1993) 251.
[16] J.F. Ziegler, J.P. Biersack, U. Littmark, The Stopping and Range of Ions in Matter, Pergamon, New York, USA, 1985.
[17] A presentation of the MDRANGE computer code is available on the World Wide Web in http://beam.helsinki.fi/~knordlun/mdh/mdh_program.html.